Induction of microRNA-155 is TLR- and type IV secretion system-dependent in macrophages and inhibits DNA-damage induced apoptosis

Manuel Koch[a], Hans-Joachim Mollenkopf[b], Uwe Klemm[c], and Thomas F. Meyer[a,1]

[a]Department of Molecular Biology, [b]Core Facility Genomics, and [c]Core Facility Experimental Animals, Max Planck Institute for Infection Biology, Berlin 10117, Germany

Edited by Carlo M. Croce, The Ohio State University, Columbus, OH, and approved March 15, 2012 (received for review October 6, 2011)

Helicobacter pylori **is a gastric pathogen responsible for a high disease burden worldwide. Deregulated inflammatory responses, possibly involving macrophages, are implicated in *H. pylori*-induced pathology, and microRNAs, such as miR-155, have recently emerged as crucial regulators of innate immunity and inflammatory responses. miR-155 is regulated by Toll-like receptor (TLR) ligands in monocyte-derived cells and has been shown to be induced in macrophages during *H. pylori* infection. Here, we investigated the regulation of miR-155 expression in primary murine bone marrow-derived macrophages (BMMs) during *H. pylori* infection and examined the downstream mRNA targets of this microRNA using microarray analysis. We report TLR2/4- and NOD1/2-independent up-regulation of miR-155, which was found to be dependent on the major *H. pylori* pathogenicity determinant, the type IV secretion system (T4SS). miR-155 expression was dependent on NF-κB signaling but was independent of CagA. Microarray analysis identified known gene targets of miR-155 in BMMs during *H. pylori* infection that are proapoptotic. We also identified and validated miR-155 binding sites in the 3′ UTRs of the targets, *Tspan14*, *Lpin1*, and *Pmaip1*. We observed that *H. pylori*-infected miR-155$^{-/-}$ BMMs were significantly more susceptible to cisplatin DNA damage-induced apoptosis than were wild-type BMMs. Thus, our data suggest a function for the prototypical *H. pylori* pathogenicity factor, the T4SS, in the up-regulation of miR-155 in BMMs. We propose the antiapoptotic effects of miR-155 could enhance macrophage resistance to apoptosis induced by DNA damage during *H. pylori* infection.**

pathogen-associated molecular pattern | mucosal immunity

The Gram-negative bacterium, *Helicobacter pylori*, is a spiral-shaped, microaerophilic pathogen that is prevalent in ∼50% of the world's population (1). This pathogen causes persistent infections of the gastric mucosa, which can result in both acute and chronic gastric diseases. Although infections frequently are asymptomatic, severe disease outcomes, such as duodenal and gastric ulcers, develop in 5–10% of infected individuals (2). Moreover, early epidemiological studies have shown a convincing association between infections with this pathogen and gastric adenocarcinoma and mucosa-associated lymphatic tissue lymphoma (3, 4). Accordingly, *H. pylori* was the first bacterial pathogen to be classified as a type I carcinogen by the World Health Organization (5). In recent years the prominent role of the bacterial genomic *cag* pathogenicity island (*cag*PAI) in severity of *H. pylori* disease has become evident. The distribution of *cag*PAI-positive *H. pylori* strains is geographically dependent; there are regions of the world where more than 95% of *H. pylori* strains (e.g., HpEast-Asia) are *cag*PAI positive, whereas strains in other regions (e.g., HpAfrica2) are *cag*PAI negative (6). The *H. pylori cag*PAI encodes the structural components of a type IV secretion system (T4SS) and a unique effector protein, cytotoxin-associated gene A (CagA). Following T4SS-mediated translocation into host cells, CagA is phosphorylated by host-cell kinases whereupon it disrupts epithelial cell function by binding to cellular phosphatases such as SHP-2 (7) and receptors such as c-met (8). Binding of the T4SS via β1-integrins also has been shown to alter signal transduction in host cells (9).

MicroRNAs (miRNAs) are small, noncoding RNAs ∼23 nt in size (10). To date, more than 600 miRNAs, which target >60% of the protein-coding genome in mammals, have been identified in humans and mice (11). Many miRNAs are transcribed as primary transcripts by RNA polymerase II. Primary transcripts are cleaved to precursor miRNAs (premiRNAs) by the RNaseIII enzyme Drosha and are exported to the cytoplasm, where further processing via Dicer RNaseIII yields mature miRNAs (12). By binding to the argonaute complex, single miRNAs can regulate a multitude of target genes by binding preferentially to the 3′ UTR of the target gene mRNA, thereby blocking translation of the mRNA and leading to mRNA degradation (13). A crucial feature for miRNA activity is based on complementarities of its seed sequence (10). miRNAs are involved in almost all cellular processes and also play crucial roles in disease, for example, in cancer. One example of a cancer-related miRNA is miR-155, which is overexpressed in different tumors, such as diffuse large B-cell lymphoma and several types of adenocarcinoma (14). This onco-miRNA also is up-regulated during *H. pylori* infection (15, 16). Targets of miR-155 include, among others, proteins of the toll-like receptor (TLR) pathway, leading, upon miR-155 induction, to attenuation of transcription factor NF-κB activity (17). Interestingly, miR-155 itself is regulated through the TLR pathway via NF-κB (18).

H. pylori can activate the NF-κB pathway by various means; however, published data are inconclusive as to how these mechanisms contribute to NF-κB signaling in general (19). In gastric epithelial cell lines, NF-κB–dependent up-regulation of IL-8 depends largely on T4SS function (20), and *H. pylori* LPS does not seem to play a crucial role in this setting (21). It has been proposed that T4SS translocation of *H. pylori* peptidoglycan activates NF-κB via the NOD1 receptor, which belongs to the cytosolic NOD-like receptor family (22). In monocyte-derived cells, such as macrophages and dendritic cells (DC), the TLR family members TLR2, TLR4, and TLR9 clearly are involved in the response to *H. pylori* infection (23). Nevertheless, discussion is ongoing as to whether *H. pylori* LPS signals via TLR4 (a common receptor for Gram-negative enterobacterial LPS) or via

Author contributions: M.K. and T.F.M. designed research; M.K., H.-J.M., and U.K. performed research; M.K. and H.-J.M. analyzed data; and M.K. and T.F.M. wrote the paper.

The authors declare no conflict of interest.

This article is a PNAS Direct Submission.

Data deposition: Microarray data presented in this paper have been deposited in the Gene Expression Omnibus (GEO) database, http://www.ncbi.nlm.nih.gov/geo/ (accession no. GSE29388).

[1]To whom correspondence should be addressed. E mail: meyer@mpiib-berlin.mpg.de.

See Author Summary on page 7144 (volume 109, number 19).

This article contains supporting information online at www.pnas.org/lookup/suppl/doi:10.1073/pnas.1116125109/-/DCSupplemental.

TLR2 (the main receptor for Gram-positive bacteria lipoteichoic acid), because *H. pylori* LPS lacks distinct features of the prototypical enterobacterial LPS (24). The RNA receptor RIG-I also has been proposed to be an intracellular receptor for *H. pylori*-mediated transcriptional activation in DCs (23).

Gram-negative bacteria may act as pro- as well as antiapoptotic factors for macrophages. For example, *Salmonella enterica* Typhimurium has been described as promoting apoptosis (25), whereas *Brucella suis* reportedly is antiapoptotic (26). *H. pylori* encodes both pro- and antiapoptotic effector molecules, such as CagA and VacA (27). Again, which factors drive the pro- or antiapoptotic response remains controversial (28, 29). In human and murine monocytic cell lines such as Raw-264.1 and THP-1, as well as in primary human monocytes, *H. pylori* was shown to induce apoptosis directly (30, 31). However, primary monocyte-derived cells seemed to be resistant to *H. pylori*-induced apoptosis (32). The antiapoptotic potential of miR-155 has been described for several cell types, including B lymphocytes (33), and in pancreatic tumors by targeting *TP53INP1* (34) and *JARID2* (35). Moreover, miR-155 has been reported to promote resistance to specific chemotherapeutics in breast cancer cells by targeting *FOXO3A* (36), and recent reports suggested proapoptotic potential of miR-155 through targeting *SKI2* in human melanoma cells (37) or *Kpc1* in murine DCs (38).

Here, we investigated the regulation of miR-155 expression by *H. pylori* in cell lines and in primary murine bone marrow-derived macrophages (BMMs) isolated from WT and gene-knockout mice. In addition to the known TLR2/TLR4-dependent up-regulation of miR-155, we found that *H. pylori* also induced miR-155 via a TLR2/TLR4-independent, T4SS-dependent mechanism in BMMs, a potentially unique function of this major pathogenicity factor. Using microarray analysis, we confirmed the miR-155–dependent down-regulation of known miR-155 gene targets during infection and validated miR-155 binding sites in the 3′ UTRs of putative miR-155 targets *Tspan14*, *Lpin1*, and *Pmaip1*. Interestingly, results in both established and putative targets suggested that miR-155 has a role in the regulation of apoptosis in macrophages during infection. Indeed, WT BMMs were more resistant than BMMs lacking miR-155 (miR-155$^{-/-}$ BMMs) to apoptosis upon cisplatin-induced DNA damage during infection, thus demonstrating the antiapoptotic function of miR-155.

Results

Up-Regulation of miR-155 Is Dependent on Multiplicity of Infection and Duration of Infection. To investigate the regulation of miR-155 in macrophages in response to *H. pylori* infection, the murine macrophage cell line J774A was infected with the mouse-adapted *H. pylori* strain Hp76. After 3 h of infection, total RNA was extracted and subjected to Northern blot. We detected up-regulation of the 65-nt premiR-155 and the 23-nt mature miR-155 form (Fig. 1*A*). Up-regulation of mature miR-155 was validated by quantitative RT-PCR (qRT-PCR) for infections with mouse-adapted strain Hp76 and the human-adapted strain P12 in comparison with mock-infected cells. The murine cell line J774A exhibited an approximately fourfold up-regulation of miR-155 during infection with both *H. pylori* strains, whereas infection of C57BL/6 WT mice BMMs (WT BMMs) resulted in an ∼20-fold up-regulation (Fig. 1*B*). To determine whether the observed effect was specific and to identify maximal induction of miR-155 expression upon infection, increasing multiplicity of infection (MOI) and an infection time course were analyzed. There was a strong correlation between MOI and the expression of miR-155 in WT BMMs after 3 h of infection with P12. Infection with an MOI of 50 showed the strongest miR-155 up-regulation, which decreased with an MOI of 10 or 1 (Fig. 1*C*). miR-155 was induced as early as 90 min postinfection (p.i.) and increased up to ∼500 fold at 30 h p.i. (Fig. 1*D*).

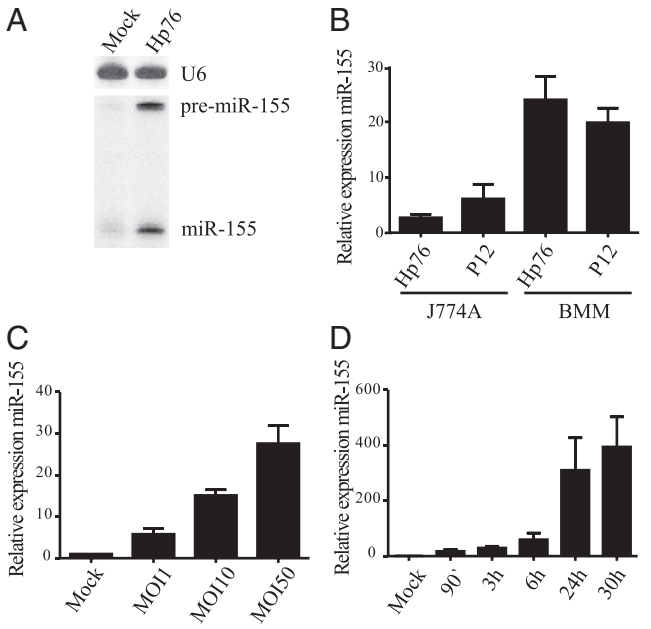

Fig. 1. Up-regulation of miR-155 by *H. pylori* in murine macrophages in an MOI- and time-dependent manner. (*A*) Up-regulation of miR-155 after 3 h of infection with the mouse-adapted strain Hp76 (MOI of 100) was determined by Northern blot in the murine macrophage cell line J774A using U6 snRNA as endogenous control. (*B*) Regulation of miR-155 by Hp76 and the human-adapted strain P12 in J774A (MOI of 100) and primary murine BMM (MOI of 50; 3 h) observed by qRT-PCR. (*C*) MOI dependency of up-regulation of miR-155 was observed by qRT-PCR in BMMs after 3 h of infection with *H. pylori* P12. (*D*) Time-course experiments reveal an increase in expression of miR-155 over the duration of infection with *H. pylori* P12 (MOI of 50) observed by qRT-PCR. The values presented here are the ΔΔCt values normalized to RnU6b snRNA as endogenous control. Experiments were performed with at least three biologically independent replicates and are presented as mean + SE.

TLR-Dependent and -Independent Up-Regulation of miR-155. Previously it has been shown that the expression and regulation of miR-155 in murine macrophages depends on ligands of the TLR family (39). It has been demonstrated that in primary phagocytes *H. pylori* can signal via TLR2, TLR4, and other members of the TLR family, leading to the release of IL-6 in a MyD88-dependent manner (23). To examine the effectors that are responsible for the observed up-regulation of miR-155, we incubated WT BMMs with TLR-specific ligands and *H. pylori* strains Hp76 and P12 for 3 h. The TLR4-specific ligand, *Escherichia coli* LPS (EC LPS), as well as the synthetic TLR2 ligand Pam3CSK4, led to an induction of miR-155 expression (Fig. 2*A*). A similar result was obtained for purified *H. pylori* P12 LPS. Heat-inactivated *H. pylori* P12 (P12 hi) and Hp76 (Hp76 hi) induced miR-155 to levels similar to that induced with viable bacteria. To ascertain whether the induction of miR-155 expression by these factors depended purely on the interaction of the main extracellular TLRs, TLR2 and TLR4, with *H. pylori* (23), BMMs isolated from C57BL/6 mice lacking receptors for both TLR2 and TLR4 (TLR2/4$^{-/-}$ BMMs) were used. These cells did not up-regulate miR-155 in response to TLR2- and TLR4-specific ligands (EC LPS and Pam3CSK4, respectively) or in response to *H. pylori* LPS (Fig. 2*B*). It has been discussed in the literature whether *H. pylori* LPS signals via TLR2 or TLR4 (40, 41). Here, we found that signaling occurred via both receptors (Fig. S1 *A* and *B*) and that signaling was absent when neither TLR2 nor TLR4 was present (Fig. 2*B*). In contrast to *H. pylori* LPS, viable *H. pylori* P12 and Hp76 showed an ∼65-fold up-regulation of miR-155 in TLR2/4$^{-/-}$ BMMs. Induction of miR-155 was even higher in TLR2/4$^{-/-}$ BMMs than in WT BMMs

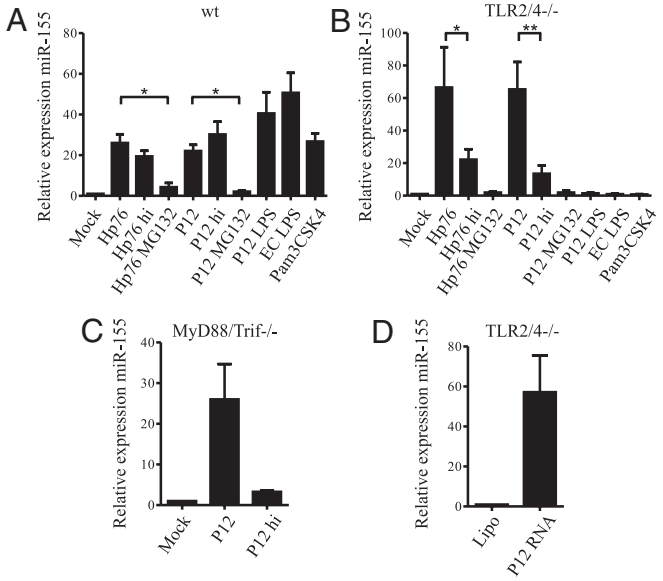

Fig. 2. TLR2- and TLR4-dependent and TLR-independent up-regulation of miR-155 by *H. pylori*. (*A*) Living and heat-inactivated (hi) *H. pylori* P12, Hp76 (MOI of 50), P12 LPS (1.5 μg/mL, 2,000 EU/mL), and the specific ligands for TLR2 (Pam3CSK4, 10 ng/mL) and TLR4 (ultra-pure *E. coli* LPS, 100 ng/mL) up-regulate miR-155 after 3 h of incubation in WT BMMs. (*B*) In BMMs lacking TLR2 and TLR4 (TLR2/4$^{-/-}$), a strong reduction of miR-155 expression can be observed using heat-inactivated *H. pylori*. The proteasome inhibitor MG-132 (10 μM) (used as an NF-κB inhibitor) almost completely abolished the up-regulation of miR-155. (*C*) The regulation of miR-155 in BMMs lacking both adaptors for TLR signaling (MyD88 and Trif) is similar to WT BMMs when using P12 (MOI of 50; 3 h). Heat-inactivation of P12 (MOI of 50) clearly reduces the up-regulation of miR-155. (*D*) The effect of transfected P12 RNA on the induction of miR-155 was tested in TLR2/4$^{-/-}$ BMMs. TLR2/4$^{-/-}$ BMMs were used to exclude contamination of P12 LPS. All data were obtained by qRT-PCR using ΔΔCt values with RnU6b or snoR-202 as endogenous control. Experiments were performed with at least three biologically independent replicates and are presented as mean + SE. Statistical significance was analyzed by Student's *t* test; $*P < 0.05$ and $**P < 0.01$.

(Fig. 2*A*). This higher induction rate can be explained by a higher endogenous basal level of miR-155 in the mock-infected WT BMMs as compared with TLR2/4$^{-/-}$ BMMs. Heat inactivation of *H. pylori* significantly reduced the relative expression of miR-155 in TLR2/4$^{-/-}$BMMs as compared with the nontreated strain, whereas the use of the proteasome inhibitor MG132 (used as an NF-κB inhibitor) completely abolished miR-155 relative expression (Fig. 2*B*). The expression of miR-155 also was investigated in BMMs lacking the adaptor proteins MyD88 or Trif (Fig. S1 *C* and *D*). MyD88 is the adaptor protein for all TLR-dependent NF-κB signaling, with the exception of TLR3- and, in part, TLR4-dependent signaling, which use the adaptor function of Trif (42). Infecting MyD88/Trif$^{-/-}$ BMMs with viable *H. pylori* led to an ∼25-fold induction of miR-155, similar to that observed with WT BMMs (Fig. 2*C*). Moreover, up-regulation of miR-155 was almost completely absent in MyD88/Trif$^{-/-}$ BMMs infected with heat-inactivated P12 (Fig. 2*C*). In the literature, *H. pylori*-derived RNA has been proposed to signal via MyD88-dependent TLRs as well as via Rig-I (23). Therefore, we tested whether transfected P12 RNA induced miR-155 in BMMs. Fig. 2*D* shows that P12 RNA strongly induced miR-155, by ∼60-fold, in TLR2/4$^{-/-}$ BMMs.

Thus, during *H. pylori* infection, miR-155 expression is induced in BMMs partially via a TLR2/4- and MyD88/Trif-dependent mechanism. However, miR-155 induction in BMMs also has a TLR-independent component that results, at least in part, from the activation of MyD88/Trif-independent pathogen-associated molecular pattern (PAMP) receptors by *H. pylori* RNA.

***H. pylori* T4SS Contributes to the Up-Regulation of miR-155.** To probe further the TLR2/4-independent component of miR-155 up-regulation, we analyzed miR-155 expression in TLR2/4$^{-/-}$ BMMs treated with bafilomycin A1 (BafA1) for 1 h before infection. BafA1 blocks the proton pump of the endosome, thereby inhibiting phagosomal maturation (43). As a result, endosomal TLRs or cytosolic receptors cannot detect *H. pylori* effectors, such as RNA (23, 44, 45). BafA1 treatment did not influence the translocation of CagA (Fig. S2). To ascertain whether BafA1 was functional in this system, up-regulation of IL-6 mRNA was quantified in TLR2/4$^{-/-}$ BMMs after *H. pylori* infection. The inhibitory effect of BafA1 on IL-6 protein expression in TLR2/4$^{-/-}$ bone marrow-derived DCs (BMDCs) has been reported previously (23) and could be confirmed here at the mRNA level (Fig. S3*A*). There was almost no expression of IL-6 mRNA in response to P12 infection in BafA1-treated TLR2/4$^{-/-}$ BMMs, whereas there was an ∼10,000-fold up-regulation of IL-6 in cells not treated with BafA1. In comparison with the abrogation of IL-6 mRNA expression in the presence of BafA1 during P12 infection, miR-155 expression was reduced by only ∼50% in BafA1-treated TLR2/4$^{-/-}$ BMMs (Fig. 3*A*) (∼25-fold up-regulation), compared with nontreated cells (∼50-fold up-regulation). Thus, to investigate the origin of the lower sensitivity of miR-155 expression to BafA1, we investigated other bacterial factors that might contribute to the miR-155 up-regulation. *H. pylori* strains Hp76 and P12ΔcagPAI (an isogenic mutant of P12), both lacking the T4SS and the CagA protein, were used for infections to confirm whether the effect was *cag*PAI dependent in TLR2/4$^{-/-}$ BMMs. *E. coli* DH1 (MOI of 10), which does not possess a T4SS, served as control. In the absence of BafA1, all infections of TLR2/4$^{-/-}$ BMMs showed very similar up-regulation of miR-155 (40- to 45-fold) (Fig. 3*A*). However, the relative expression of miR-155 decreased by ∼50% in TLR2/4$^{-/-}$ BMMs during infection with the T4SS-positive strain P12, as previously shown in the presence of BafA1. The effect of BafA1 was significantly larger in strains that lacked the T4SS (Hp76, P12ΔcagPAI, and *E. coli* DH1): miR-155 expression was reduced by ∼80% in the presence of BafA1. The reduced capacity of T4SS-negative strains to induce miR-155 expression in the presence of BafA1 compared with T4SS-positive strains was highly significant ($P < 0.001$), thus implying that the TLR2/4-independent expression of miR-155 contains a T4SS-dependent component. This effect of BafA1 was not observed in WT BMMs, where the TLR-dependent miR-155 expression likely was dominant (Fig. S3*B*). This result led us to question whether the observations were dependent only on the presence of the T4SS or also were dependent on T4SS function and CagA. To gain further insights into this process, infections were performed with isogenic mutants of P12 lacking either the CagA protein (P12ΔcagA) or the CagL protein (P12ΔcagL), which is reported to be located at the tip of the T4SS and the absence of which renders the T4SS nonfunctional (46). In all mutants tested, cells not treated with BafA1 did not differ significantly from WT P12 cells in miR-155 up-regulation (40- to 50-fold up-regulation). However, the up-regulation of miR-155 was reduced significantly ($P < 0.01$) in BafA1-treated TLR2/4$^{-/-}$ BMMs infected with the P12ΔcagL mutant as compared with WT P12; levels were comparable to those observed with the P12ΔcagPAI strain (Fig. 3*B*). By contrast, the P12ΔcagA mutant behaved similarly to WT P12 (Fig. 3*B*). These experiments strongly suggested that, although the observed miR-155 expression in BMMs was partially dependent on the T4SS, this process was independent of CagA. Given reports showing that *H. pylori* peptidoglycan leads to NF-κB translocation in epithelial cells via NOD1 (22), we tested the potential of the NOD1- and NOD2-specific ligands TriDAP and MDP, respectively, to induce miR-155. We found no NOD1 ligand-mediated up-regulation of miR-155 in TLR2/4$^{-/-}$ BMMs (Fig. S4*B*); however a slight up-regulation of miR-155 via NOD2 could be observed at high

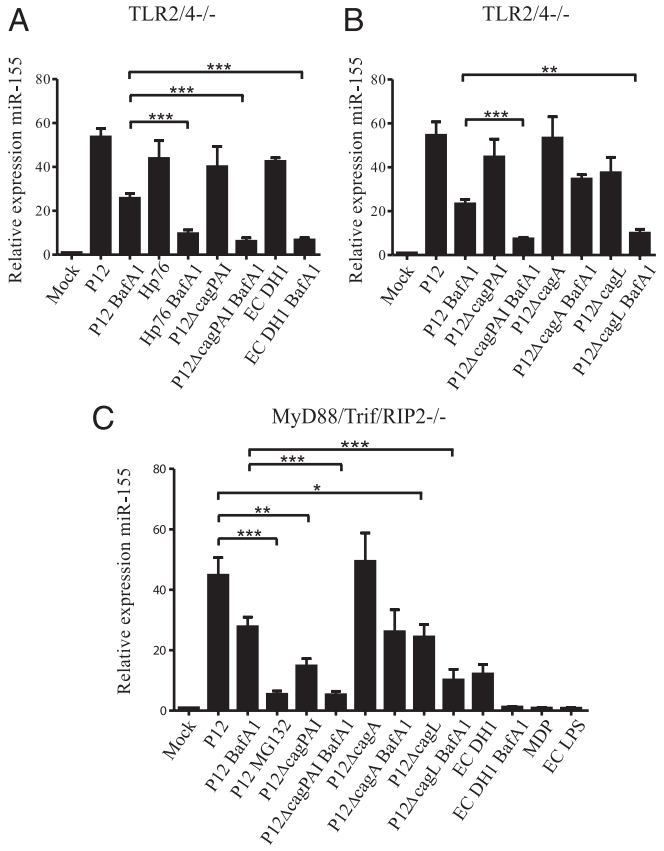

Fig. 3. Regulation of miR-155 is dependent on the T4SS. (*A*) Blocking phagosomal maturation by BafA1 (100 nM) 1 h before infection decreases miR-155 upregulation in TLR2/4$^{-/-}$ BMMs infected (3 h) with P12 (MOI of 50) but not as strongly as in BafA1-treated BMMs infected with Hp76 (MOI of 50) or P12ΔcagPAI (MOI of 50), both of which lack the *cag*PAI. Similar inhibition can be observed for BafA1-treated cells infected with *E. coli* DH1 (MOI of 10). (*B*) BafA1 treatment inhibits the up-regulation of miR-155 significantly more during infection of TLR2/4$^{-/-}$ BMMs with the P12ΔcagL mutant (MOI of 50; 3 h) than with the P12ΔcagA (MOI of 50) mutant. The response to P12ΔcagL is similar to that to P12ΔcagPAI, whereas the response to P12ΔcagA is similar to that to WT P12. (*C*) MyD88/Trif/Rip2$^{-/-}$ BMMs were pretreated with BafA1 (100 nM) or were left untreated, then were infected for 3 h with P12, P12 P12ΔcagPAI, P12ΔcagA, or P12ΔcagL (all MOI of 50), and were checked for the expression of miR-155. In addition, these cells were infected with *E. coli* DH1 for 3 h (MOI of 10). As controls, MDP (100 μg/mL) and EC LPS (100 ng/mL) were used. All data presented here are from qRT PCR experiments. Data are ΔΔCt values using snoR-202 as endogenous control and the mock-infected control to normalize. Experiments were performed with at least three biologically independent replicates and are presented as mean + SE. Statistical significance was analyzed by Student's *t* test; $*P < 0.05$; $**P < 0.01$; $***P < 0.001$.

concentrations of MDP. Additionally, BMMs lacking Rip2 [thus lacking NOD-dependent NF-κB activation (47)] showed up-regulation of miR-155 upon P12 infection (~60 fold) similar to that in infected TLR2/4$^{-/-}$ BMMs (Fig. S4*A*). Because the T4SS-mediated effect may be explained by the translocation of peptidoglycan, we generated a mouse mutant lacking MyD88/Trif/Rip2$^{-/-}$ and tested the expression of miR-155 in BMMs derived from these mice. MyD88/Trif/Rip2$^{-/-}$ BMMs did not up-regulate miR-155 upon EC LPS or MDP stimulation, demonstrating that TLR as well as the NOD1/2 signaling truly was abrogated in these cells. However, when we infected MyD88/Trif/Rip2$^{-/-}$ BMMs with *H. pylori* P12, a strong (45-fold) up-regulation of miR-155 could be observed (Fig. 3*C*). Pretreatment with BafA1 reduced this up-regulation of miR-155 to ~27-fold, and pretreatment with MG132 further diminished miR-155 induction to approximately fivefold. In *H. pylori* P12ΔcagPAI without BafA1 pretreatment, miR-155 induction was reduced significantly compared with WT P12, possibly as a direct result of the absent T4SS-dependent activation. Pretreatment with BafA1 further decreased the up-regulation of miR-155 in these BMMs. The P12ΔcagA mutant up-regulated miR-155 expression to levels comparable with WT P12 (in both, an ~50-fold miR-155 induction) during infection of MyD88/Trif/Rip2$^{-/-}$ BMMs. By contrast, P12ΔcagL showed a reduction of miR-155 up-regulation (~50% of that in WT P12 cells). Pretreatment with BafA1 significantly decreased miR-155 up-regulation of P12ΔcagL-infected MyD88/Trif/Rip2$^{-/-}$ BMMs. Thus, NOD1/2 signaling can up-regulate miR-155 expression weakly in BMMs, but the T4SS-dependent regulation of miR-155 expression during *H. pylori* infection is independent of NOD1/2 signaling.

Downstream Effects of miR-155 During *H. pylori* Infection. To investigate the role of miR-155 in primary macrophages during infection with *H. pylori* P12, BMMs from WT mice were infected for 6 h and then cultivated in differentiation medium containing gentamycin for another 24 h to detect targets down-regulated by miR-155 without affecting the survival of the cells. The up-regulation of miR-155 at this time point (30 h p.i.) had been determined previously (Fig. 1*D*). A microarray analysis of total mRNA was performed with mock-infected WT BMMs and P12-infected WT BMMs (array 1). Additionally, P12-infected WT BMMs were compared with P12-infected BMMs isolated from miR-155$^{-/-}$ mice (miR-155$^{-/-}$ BMMs) completely lacking miR-155 expression (array 2). The numbers of regulated genes are depicted in Fig. 4*A*. To identify direct targets of miR-155, hits with a cutoff of a 1.5-fold change and a *P* value <0.00001 that were down-regulated in WT P12 infected BMMs relative to miR-155$^{-/-}$ BMMs were examined for their putative miR-155 binding sites as predicted by TargetScan5.1 (48). Overall, 8.5% (1,234 of 14,506) of genes spotted on the array were predicted putative targets of *Mus musculus* (mmu)-miR-155 (for genes excluded, see *Materials and Methods*). Comparison of *H. pylori* infected WT BMMs with *H. pylori* infected miR-155$^{-/-}$ BMMs resulted in 17.9% (82/458) of all down-regulated genes with a cutoff of a 1.5-fold change and a *P* value < 0.00001 that contained a 7-mer or 8-mer complementary to the seed region of mmu-miR-155 (Fig. 4*B*). Statistical analysis (χ^2) showed this gene set to be significantly enriched in targets of mmu-miR-155 ($P < 0.0001$) and highlighted that miR-155 exerts a strong effect on the overall regulation in response to P12 infection. Direct targets of miR-155 were considered to be down-regulated in WT relative to miR-155$^{-/-}$ BMMs; however, these targets still can be either unregulated or differentially regulated in mock-infected and infected WT BMMs (array 1). We subsequently focused only on the subset of genes that were down-regulated on both arrays to observe the direct biological link between *H. pylori* infection and the role of miR-155. Overall, 128 genes were down-regulated and overlapping on both arrays with a cutoff of 1.5-fold change and a *P* value < 0.00001. Table S1 depicts 35 of these mRNAs that have at least one miR-155 binding site in their 3′ UTR as identified by TargetScan5.1 (i.e., 35 genes are down-regulated in an *H. pylori*- and miR-155–dependent manner as putative direct targets). This result represented a further significant enrichment of miR-155 targets by 27.3% (35/128) (Fig. 4*B*) as determined by χ^2 statistics ($P = 0.0422$).

Validation of Direct Targets of miR-155. Some of the direct miR-155 targets identified by our analysis have been published previously, namely, *Bach1*, *Trp53inp1*, *Smad5*, and *Map3k7ip2* (34, 49–51). We additionally identified the putative targets *Tspan14*, *Lpin1*, and *Pmaip1*. To examine further the microarray data and the direct link between miR-155 and *H. pylori* infection, we validated

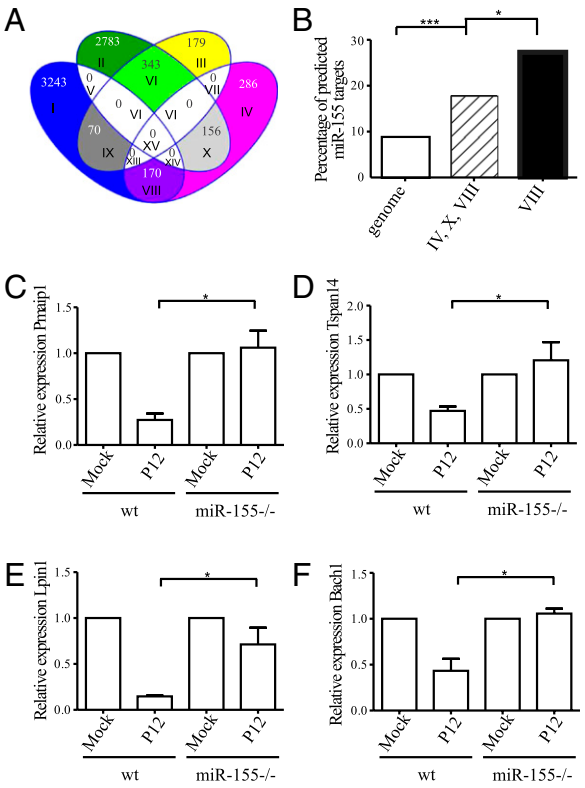

Fig. 4. mRNA microarray analysis of P12-infected BMMs lacking miR-155 shows enrichment of miR-155 targets. (*A*) Venn diagram representing differentially regulated genes on array 1 (P12 infected WT BMMs relative to mock-infected WT BMMs) and array 2 (P12 infected WT BMMs relative to miR-155$^{-/-}$ BMMs). Infections were for 30 h using MOI of 50. A total of 6,765 and 1,204 genes were regulated differentially in array 1 and array 2, respectively. Array 1: Groups II, VI, and X contain up-regulated genes; groups I, IX, and VIII contain down-regulated genes. Array 2: Groups III, VI, and IX contain up-regulated genes; groups IV, X, and VIII contain down-regulated genes. Group VIII contains genes down-regulated in both array 1 and array 2. (*B*) Comparison of all predicted targets of TargetScan (conserved and nonconserved) and all genes on the microarray (genome) with the down-regulated genes in array 2 (IV, X, VIII) reveals a significant bias toward miR-155 target genes when performing χ^2 statistics ($P < 0.0001$). The enrichment is even higher in the overlapping down-regulated genes of arrays 1+ 2 (VIII) (χ^2 test, $P = 0.0422$). (*C–F*) Validation of regulated mRNAs from the microarray by qRT-PCR. Only in the WT BMMs were targets significantly down-regulated compared with miR-155$^{-/-}$ BMMs. Relative values presented here are ΔΔCt values normalized to β-Actin as an endogenous control and a mock-infected control. Experiments were performed with at least three biologically independent replicates and are presented as mean + SE. Statistical significance was analyzed by Student's *t* test; *$P < 0.05$; ***$P < 0.001$.

the putative targets that contained two binding sites for mmu-miR-155 (*Tspan14*, *Lpin1*, and *Pmaip1*) together with *Bach1* by qRT-PCR. These putative targets were down-regulated in P12-infected WT BMMs but were largely unregulated in P12-infected miR-155$^{-/-}$ BMMs (Fig. 4 *C–F*). To identify the direct effect of miR-155 on these newly identified targets, the 3′ UTRs (possessing two mmu-miR-155 binding sites) were cloned into the 3′ region of a Renilla luciferase reporter plasmid containing firefly luciferase as endogenous control (52–56). In addition, the predicted seed regions (7-mer or 8-mer) of the binding sites were mutated from UUA to AAU. For *Tspan14* a full-length (Tspan14-2) and a truncated deletion of the 3′ UTR missing the last 83 nt (Tspan14-1) were used. Tspan14-2 contained two mmu-miR-155 binding sites, whereas the truncated version (Tspan14-1) contained only one that subsequently was mutated (Fig. S5). *Lpin1* and *Pmaip1* both contained two binding sites for mmu-miR-155, both of which were mutated (Fig. S5). These vectors then were transfected into HEK293T cells together with the precursor of mmu-miR-155 (premmu-miR-155) and a non-specific control, prehsa-miR-198 (human). Cotransfection of premmu-miR-155 with the respective plasmids containing the 3′ UTR of the putative targets *Pmaip1*, *Tspan14*, and *Lpin1* showed a strong down-regulation of the luciferase activity of the Renilla luciferase normalized to firefly luciferase (Fig. 5 *A–C*). Mutating the first predicted mmu-miR-155 binding site led to a significant recovery of the Renilla activity of Pmaip1-3′ UTR and Lpin1-3′ UTR, and mutating both binding sites led to almost full recovery of the Renilla luciferase signal; these results indicated that both mmu-miR-155 binding sites needed to be deactivated. For Tspan14 the truncated version (Tspan14-1) exhibited significantly increased Renilla luciferase activity compared with Tspan14-2 when cotransfected with premmumiR-155, whereas mutating the predicted binding site in Tspan14-1 restored the Renilla luciferase signal almost completely. By mutating the mmu-miR-155 putative binding sites of our identified targets, we propose a miR-155–mediated regulation of the genes *Tspan14*, *Pmaip1*, and *Lpin1*.

Cisplatin-Induced Apoptosis Is Inhibited by miR-155. A functional analysis using Ingenuity Pathway Analysis software was performed with the 35 genes listed in Table S1. Interestingly, 39.4% of those genes were cell death related, whereas, in a control set comprising genes differentially regulated in mock- vs. P12-

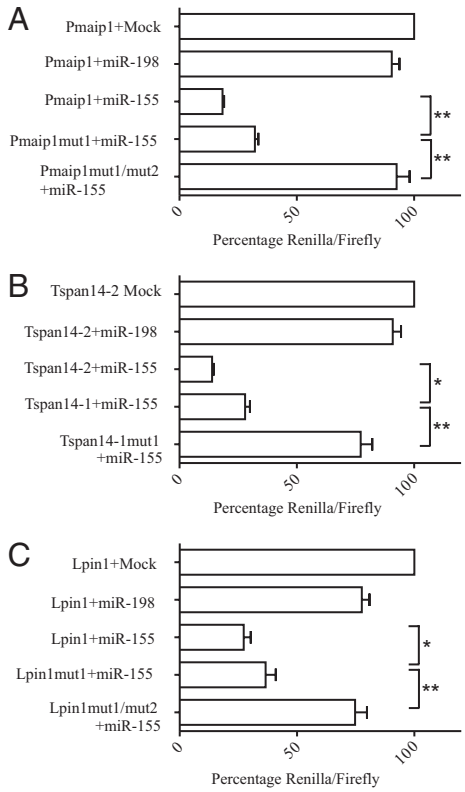

Fig. 5. Validation of direct targets of mmu-miR-155. The 3′ UTRs of the putative targets Pmaip1 (*A*), Tspan14 (*B*), and Lpin1(*C*) were cloned in the 3′ direction to Renilla luciferase in a luciferase reporter plasmid containing Renilla and firefly luciferase as internal control. The putative binding sites subsequently were mutated in the seed region of the miRNA. The UUA motif (nucleotides 2–4) was replaced by AAU. The data are luciferase assays normalized to the untreated plasmid. All experiments were performed with at least three independent experiments and are presented as mean + SE. Statistical significance was analyzed by Student's *t* test; *$P < 0.05$; **$P < 0.01$.

infected WT BMMs, only 27.4% of the genes were cell death related. Together with this finding, a large proportion of the genes (Table S1) are implicated in DNA damage responses (e.g., the known miR-155 targets *Bach1*, *Trp53inp1*, and *MAP3K7ip2* and, although less well-established, our identified targets, *Pmaip1*, and *Lpin1*). Cisplatin is a well-known drug that induces apoptosis via DNA damage and has been shown previously to up-regulate LPIN1, PMAIP1, and TRP53INP1 (57). Accordingly, cisplatin was tested on P12-infected WT BMMs and miR-155$^{-/-}$ BMMs to elucidate the potential role of miR-155 in apoptosis mediated by DNA damage. As readouts, cleavage of Procaspase-3 to activated apoptosis effector Caspase-3 and the cleavage of the Caspase-3 downstream target poly(ADP ribose) polymerase (PARP) were analyzed by Western blot. BMMs were infected for 6 h and incubated further for another 24 h to emphasize miR-155-dependent effects. Following 18 h of cisplatin treatment, substantial apoptosis was observed in mock-infected cells, whereas the induction of apoptosis mediated by DNA damage was inhibited in WT BMMs infected with *H. pylori* P12 (Fig. 6*A*). This result is in contrast to that seen in P12-infected miR-155$^{-/-}$ BMMs, which had PARP/Procaspase-3 cleavage levels comparable to those of mock-infected cells. The quantification of six independent Western blots is shown in Fig. 6 *B* and *C*. For further confirmation, Caspase-3/-7 activity was measured using proluminescent Caspase-3/-7 substrate (Fig. 6*D*). As a control, water-soluble tetrazolium salts (WST-8) assays were performed before cisplatin treatment; no difference between the WT and miR-155$^{-/-}$ cells could be detected (Fig. S6). Finally, during infection, Caspase-3/-7 activity was higher in miR-155$^{-/-}$ than in WT BMMs, further emphasizing the differences in apoptosis and the biological impact of miR-155.

Discussion

Here we demonstrate a TLR- and NOD1/2-independent up-regulation of miR-155 in macrophages during *H. pylori* infection. The TLR-dependent up-regulation of miR-155 via MyD88 and Trif in BMMs has been reported previously (39); here, however, we show there is a TLR-independent up-regulation of miR-155 by *H. pylori* in macrophages occurring via the NF-κB pathway. The T4SS-dependent up-regulation of miR-155 in macrophages that we report confirms the importance of this microRNA in *H. pylori* infection and may be of particular relevance in the context of suboptimal TLR activation, resulting in part from reduced MyD88/Trif expression, in gastrointestinal macrophages (58).

We found that the signaling pathway upstream of miR-155 during *H. pylori* infection appeared to differ from that of other NF-κB–dependent genes, such as IL-6. IL-6 mRNA synthesis was almost completely dependent on MyD88 and abolished by BafA1 treatment of TLR2/4$^{-/-}$ BMMs, consistent with previous data (23). By comparison, miR-155 expression during infection was less sensitive to BafA1 treatment in TLR2/4$^{-/-}$ BMMs and led us to investigate the role of other bacterial factors in the regulation of miR-155 expression during infection. The up-regulation of miR-155 was significantly stronger in T4SS-positive strains than in T4SS-negative strains when extracellular TLR activation/signaling was blocked (TLR2/4$^{-/-}$ BMMs) in con-

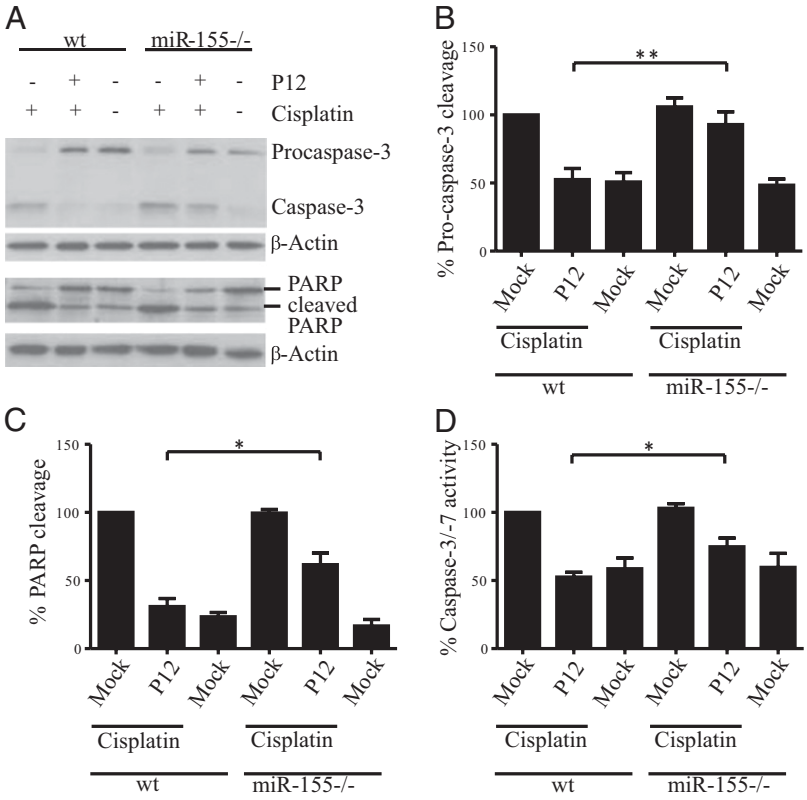

Fig. 6. Up-regulation of miR-155 in *H. pylori*-infected BMMs blocks cisplatin-induced apoptosis. (*A*) Pro-caspase-3 and PARP cleavage was detected by Western blot after *H. pylori* infection (MOI of 50) and 18 h of treatment with cisplatin (50 μM). Here, cleaved Procaspase-3 and PARP can be observed in the cisplatin-treated mock-infected BMMs but not in the untreated cells. Procaspase-3 as well as PARP cleavage is inhibited after infection but, as seen in the quantification in *B* and *C*, is inhibited significantly less in the miR-155$^{-/-}$ BMMs than in WT BMMs. The blot in *A* is representative of six biologically independent experiments, and quantification shows the mean + SE of six biologically independent experiments. (*D*) The activity of caspase-3/-7 was determined by a luciferin-based assay. The activity is less in the P12-infected WT BMMs than in P12-infected miR-155$^{-/-}$ BMMs. Experiments were performed with at least three biologically independent replicates and are presented as mean + SE. Statistical significance was analyzed by Student's *t* test; $*P < 0.05$; $**P < 0.01$.

junction with a block to endosomal maturation (BafA1 treatment) and/or in macrophages devoid of all MyD88/Trif-dependent TLR signaling and NOD1/2 activation (MyD88/Trif/Rip2$^{-/-}$). Notably, the *H. pylori* CagA protein itself has been reported to induce NF-κB signaling directly in gastric epithelial cells (59); however, we found that the T4SS-dependent miR-155 up-regulation was independent of this major effector protein. Induction of NF-κB by *H. pylori* also has been proposed to occur via NOD receptors (22). We have shown here that classical NOD ligands have limited capacity to induce miR-155 in macrophages; however, the T4SS-dependent miR-155 up-regulation during infection was independent of NOD1/2 receptor activity, as demonstrated by the use here of MyD88/Trif/Rip2$^{-/-}$ BMMs. The MyD88/Trif-independent up-regulation of miR-155 observed here displays a phenotype similar to that seen with the induction of TNF-α and type I IFNs or IFN-induced genes, such as *CXCL10*, demonstrated for intestinal bacteria-infected BMMs (60, 61). IFN-β and TNF-α incubation induced miR-155 expression; however, induction of miR-155 by TLR ligands still occurred in the absence of TNF receptors and IFN-α receptors in BMMs (39). In accordance with our data, a partial SPI1/2 (encoding *Salmonella* translocated effector proteins and a type III secretion system)-dependent effect in the up-regulation of miR-155 in LPS tolerized macrophages has been demonstrated during *Salmonella enterica* Typhimurium infection (54). We speculate that the T4SS-dependent pathway could be triggered by an as yet unknown T4SS translocated effector, which is detected by cytosolic receptors in BMMs, or could result from docking of the T4SS to an unidentified plasma membrane receptor(s). Alternatively, the *H. pylori* T4SS could signal directly via members of the integrin family, e.g., integrin β1 receptors (62). Indeed, downstream effects of this interaction have been described previously (46). To our knowledge the TLR- and NOD1/2-independent regulation of an inflammatory response via NF-κB during bacterial infection has not been reported previously. The T4SS-dependent effect shown here contributes to the ongoing discussion as to whether the bacterial secretion system machinery is involved directly in innate immune detection and responses of professional phagocytes, as shown for *Legionella pneumophila* and *Yersinia pseudotuberculosis* (47, 61). Recently, the question of the existence of "vita-PAMPs," which implicates pattern recognition from live rather than dead bacteria, has been addressed (63). Our study contributes to this discussion in that the functional *H. pylori* T4SS could resemble such a vita-PAMP. We anticipate that the MyD88/Trif/Rip2$^{-/-}$ generated here will have future applications for investigations into the contribution of bacterial secretion system to the activation of PAMP receptors.

As recently suggested, *H. pylori* is found not only on the epithelial cell surfaces of the infected gastric mucosa but also in the lamina propria inside mucosal macrophages that are located directly basally of epithelial cells (64). One hypothesis for the mechanism of *H. pylori*-induced pathology is that during persistent infection an unresolved inflammatory response, possibly involving macrophages, contributes to severity of disease. Depletion of macrophages in vivo has been suggested to confer protection against gastritis in the presence of high bacterial loads (65). We previously reported that miR-155 was up-regulated in gastric biopsies of human volunteers infected with *H. pylori* for 80 d, and a major infiltration of macrophages/DCs was detected at the RNA level (15). In addition, we recently reported that miR-155 expression is important for T-helper cell 1/17 immunity to *H. pylori* infection in vivo, because miR-155$^{-/-}$ T cells impaired the ability of mice to control bacterial load; interestingly, miR-155$^{-/-}$ mice also were protected against pathology induced by *H. pylori* infection (66). We now report that, in addition to its role in T-cell immunity, miR-155 also has a role in resistance to apoptosis caused by DNA damage in macrophages. It is conceivable that increased macrophage survival in the inflammatory environment could contribute to the phenotype of *H. pylori* infection observed in vivo (66).

We observed remarkable gene-regulatory patterns for miR-155 in BMMs during *H. pylori* infection and strong enrichment of numerous miR-155 targets, both those identified here and previously published (34, 49–51), demonstrating the importance of miR-155 during infection. Our data show the substantial impact of a single miRNA on the overall mRNA expression profile during infection. Validation of several microarray hits by qRTPCR showed not only that the respective target RNAs were down-regulated during infection with *H. pylori* in WT BMMs but also that this down-regulation was attenuated almost completely in miR-155$^{-/-}$ BMMs. Overall, there was a significant enrichment in target genes with established roles in determining cell fate (e.g., regulation of apoptosis/DNA damage). In particular, the targets *TRP53INP1*, *BACH1*, and *Map3k7ip2* (*TAB2*) (34, 50, 51) were confirmed here as being regulated by miR-155 in murine macrophages and have been reported to be regulated in response to DNA damage (67–69). Three highly regulated genes with two 3′ UTR miR-155 binding sites were selected on the basis of their novelty as miR-155 targets and were validated in depth. These targets, *Lpin1* (70), *Pmaip1* (57), and *Tspan14* (71, 72), have reported roles in cell survival/DNA damage, but these roles are not as well established as those of many other targets of miR-155 that we identified from our screen. Interestingly however, it has been demonstrated that Pmaip1/Noxa$^{-/-}$ BMMs were more resistant than WT BMMs to apoptosis induced by vaccinia virus Ankara (73). Our experiments revealed that *H. pylori*-infected WT BMMs are substantially more resistant than mock-infected control cells to apoptosis induced by DNA damage. *H. pylori*-infected miR-155$^{-/-}$ BMMs were almost as sensitive as mock-infected BMMs to apoptosis. Previous reports suggested a direct induction of apoptosis by *H. pylori* in monocyte-derived cell lines (30, 31). However, in line with our results, others detected no apoptosis in murine BMDCs without sensitization (32), and *H. pylori* blocked apoptosis induced by DNA damage in Mongolian gerbils (74). In addition, it has been reported that the overall effect of miR-155 may be antiapoptotic/chemoresistant, thereby explaining the high expression of miR-155 in different tumor types (14, 36). Again, this suggestion is in agreement with the results obtained here. It is possible that miR-155 helps stabilize macrophages in the strongly inflammatory environment created during *H. pylori* infection. Indeed, DNA damage triggered by nitric oxide or reactive oxygen species has been observed in *H. pylori*-infected patients (75). It has also been reported that in inducible nitric oxide synthase double-knockout mice infected with *H. pylori*, gastric epithelial cells do not exhibit DNA damage and apoptosis to the same extent as in *H. pylori*-infected WT mice (76). This and other mechanisms of DNA damage may lead to apoptosis in the surrounding tissue (77), which may contribute to the pathology of *H. pylori* infections.

Materials and Methods

Cell Culture and Generation of BMMs. Murine J774A.1 (ACC170; Deutsche Sammlung von Mikroorganismen und Zellkulturen) cells were grown in RPMI medium (Gibco) containing 10% (vol/vol) heat-inactivated FCS. BMMs were generated as described elsewhere (78). In brief, monocytes were isolated from the femur and tibia of C57BL/6 mice and were plated in 10-cm dishes in RPMI medium containing 10% (vol/vol) heat-inactivated FCS and 30% (vol/vol) L929 supernatant as source of macrophage colony-stimulating factor. After 7 d in culture these cells were washed twice with PBS and were replated overnight in RPMI medium containing 10% (vol/vol) heat-inactivated FCS and 10% (vol/vol) L929 supernatant. Purity of the culture was controlled by CD11b^{+} and F4/80^{+} antibodies in FACS analysis with the respective isotype control (both from RnD Systems).

Bacterial Culture and Infection Experiments. *H. pylori* P12 (strain collection no. 243) and its isogenic mutants P12ΔcagPAI (no. P387), P12ΔcagL (no. P454),

and P12ΔcagA (no. P378) were cloned as described previously by replacing the gene with a chloramphenicol or kanamycin cassette (79) and were grown on GC agar plates as described elsewhere (79). Infection was carried out after 3 h of serum starvation in RPMI medium with the respective MOI and time point. Cells were serum starved for the duration of infection, except for the late time points 24 h and 30 h, at which medium was replaced with RPMI, 10% (vol/vol) heat-inactivated FCS, 10 μg/mL gentamicin (Sigma) (at 24 h), and 10% (vol/vol) L929SN (at 30 h). Heat-inactivation of bacteria was performed at 56 °C for 1 h. P12 LPS was purified by the hot phenol-water technique as previously described (80) followed by octyl-Sepharose column, DNaseI, RNaseA, and proteinase K treatment (40). Activity and concentration of P12 LPS was tested by LAL Pyrochrome assay (Pyroquant). P12 RNA was purified with the RNeasy RNA purification kit with on-column DNA digestion (Qiagen). The RNA was transfected with Lipofectamine 2000 (Invitrogen) according to the manufacturer's protocol. *E. coli* strain DH1 (No. E60) was grown in LB liquid culture and used for experiments in the logarithmic growth phase.

Reagents. For stimulations, the TLR4 ligand ultrapure *E. coli* LPS, the NOD1 ligand TriDAP, the NOD2 ligand MDP (all from Invivogen), and the synthetic TLR2 ligand Pam_3CSK_4 (EMC Microcollections) were used. As inhibitors the proteasome inhibitor MG132 (C2211) and the inhibitor of endosomal maturation Bafilomycin A1 (B1793) (both from Sigma) were used. Cisplatin (Calbiochem), Bafilomycin A1, and MG132 were dissolved in DMSO to final concentrations of 50 μM, 100 nM, and 50 μM, respectively.

RNA Isolation and qRT-PCR. Total RNA was isolated by the TRIzol (Invitrogen) method following the manufacturer's protocol. The qRT-PCR for the quantification of miRNAs was performed according to the manufacturer's protocol (Applied Biosystems) in two steps using specific primers for mmu-miR-155 (Assay ID: 001806), RnU6b (Assay ID: 001093), or snoR-202 (Assay ID: 001232). In total, 10 ng RNA was used for reactions. Relative expression levels were determined by applying the ΔΔCt method (81) using snoR-202 or RnU6b as endogenous controls and normalization to mock-infected cells.

For the detection of mRNAs, the one-step SYBR-green method using the RNA-to-Ct assay was followed in accordance with the manufacturer's protocol (Applied Biosystems). Ten nanograms of RNA were used for each reaction. Relative expression levels were determined by applying the ΔΔCt method using β-Actin as endogenous control and normalization to the mock-infected cells. Primer sequences are given in Table S2.

Northern blotting was performed according to ref. 54.

Luciferase Assay. The 3′ UTRs from the genes *Lpin1*, *Tspan14*, and *Pmaip1* were cloned from murine BMM genomic DNA 3′ to the Renilla luciferase psicheck2 vector (Promega) between the XhoI and NotI restriction sites. This plasmid also contained firefly luciferase as an endogenous control. To identify miR-155 binding sites, mutagenesis experiments were performed using the psicheck2-Lpin1, psicheck2-Pmaip1, and psicheck2-Tspan14-1 vectors as template. The mutagenesis experiments were performed with the Phusion polymerase (Finnzymes) according to the manufacturer's protocol, followed by a 3-h DpnI digestion (Fermentas) at 37 °C. Selected clones were controlled by plasmid-specific sequencing. Primer sequences are given in Table S2.

These plasmids were transfected into HEK293T cells (P4-8) at a virtual confluency of 70%; plasmids (1 μg/mL) were incubated with Lipofectamine 2000 (Invitrogen) and the respective precursors of miRNAs [(mmu-miR-155) (AM17100 ID: PM13058; Ambion), hsa-miR-198 (AM 17100 ID: 11088; Ambion)] or controls, according to the manufacturer's protocol. HEK293T cells were incubated for 24 h; then the Dual-Glo Luciferase assay was performed according to the manufacturer's protocol (Promega).

Microarray Analysis. Microarray experiments were performed as dual-color hybridizations. To compensate for dye-specific effects, an independent dye-reversal color swap was applied. Quality control and quantification of total RNA was assessed using an Agilent 2100 Bioanalyzer (Agilent Technologies) and a NanoDrop 1000 UV-Vis spectrophotometer (Kisker). RNA labeling was performed with the dual-color Quick-Amp Labeling Kit (Agilent Technologies). In brief, mRNA was reverse transcribed and amplified using an oligo-dT-T7 promoter primer, and resulting cRNA was labeled with Cyanine 3-CTP or Cyanine 5-CTP. After precipitation, purification, and quantification, 1.25 μg of each labeled cRNA was fragmented and hybridized to whole-mouse genome 4 × 44k multipack microarrays (AMADID 014868) according to the supplier's protocol (Agilent Technologies). Scanning of microarrays was performed with 5-μm resolution using a G2565CA high-resolution laser microarray scanner (Agilent Technologies) with XDR extended range. Raw microarray image data were analyzed with the Image Analysis/Feature Extraction software G2567AA v. A.10.5.1 (Agilent Technologies) using default settings and the GE2_105_Jan09 protocol. The extracted MAGE-ML files were analyzed further with the Rosetta Resolver Biosoftware, Build 7.2.2 SP1.31 (Rosetta Biosoftware). Ratio profiles comprising single hybridizations were combined in an error-weighted fashion to create ratio experiments. A 1.5-fold change expression cutoff for ratio experiments was applied together with anti-correlation of ratio profiles, rendering the microarray analysis highly significant ($P < 0.01$), robust, and reproducible. Microarray data presented in this paper have been deposited in the National Center for Biotechnology Information Gene Expression Omnibus (GEO; http://www.ncbi.nlm.nih.gov/geo/) and are accessible through GEO Series accession no. GSE29388.

Data Analysis. To analyze the microarray results further, all regulated genes were compared with the predicted targets of mmu-miR-155 by TargetScan5.1 (48). Because TargetScan5.1 predicts only targets with RefSeq mRNA accession numbers, only genes with a RefSeq accession number were used. In total, the microarray contained 14,506 genes with RefSeq accession numbers. From those genes a set-union of 1,234 genes were matched with conserved and nonconserved mmu-miR-155 predicted targets that also were identified by the microarray analysis. For identification of targets, a cutoff of 1.5-fold change and $P < 0.00001$ was used. For statistical analysis χ^2 statistics were performed. Biological effects of target genes with RefSeq numbers were analyzed subsequently with the Ingenuity Pathway Analysis software package.

Apoptosis Assays. BMMs were grown in RPMI medium containing 10% (vol/vol) heat inactivated FCS plus 10% (vol/vol) L929 supernatant (standard medium). These cells were infected with *H. pylori* P12 (MOI of 50) for 6 h in RPMI only; then the medium was replaced by standard medium containing gentamicin, and incubation continued for a further 24 h. After incubation, apoptosis was induced using 50 μM cisplatin for 18 h in RPMI containing 10% (vol/vol) heat-inactivated FCS. Samples were taken for Western blot and for Caspase-Glo-3/-7 assays (Promega). To check for cell viability the WST-8 assay according to the Colorimetric Cell Viability Kit I assay (Promokine) was performed.

Western Blot and Quantification. For Western blot, Laemmli buffer was added directly to BMMs. Depending on the protein of interest, 5–15% SDS/PAGE gels (CagA: 5%, PARP: 10%, Caspase-3: 15%) were used for blotting onto a PVDF membrane. After blotting, membranes were blocked with TBS buffer containing 0.1% (vol/vol) Tween-20 and 3% (wt/vol) BSA. Antibodies and dilutions were as follows: rabbit anti-Caspase-3, 1:1,000 (9662; Cell Signaling); rabbit anti-PARP, 1:1,000 (sc-7150; Santa Cruz); mouse anti–β-Actin, 1:3,000 (A5441; Sigma); rabbit anti-pY99, 1:1,000 (sc-7020, Santa Cruz); rabbit anti-CagA, 1:1,000 (sc-25766, Santa Cruz); rabbit anti-IQGAP, 1:1,000 (sc-10792; Santa Cruz); sheep anti-mouse HRP, 1:3,000 (NA931V; Amersham); donkey anti-rabbit HRP, 1:3,000 (NA934V′ Amersham). ECL Western blotting substrate either was detected by Hyperfilm ECL (Amersham) or quantified using ImageQuant LAS4000 (GE) (for the apoptosis assay). Signals detected by ImageQuant LAS4000 were maintained below saturation, and images were not contrast adjusted before AIDA Image Analysis (Raytest). All signals were marked with the same pixel size, and densities were determined by AIDA. The 2D region report was analyzed further and normalized to the WT BMM mock-infected cisplatin-treated cells.

Mice. Mice were bred and maintained according to German and European guidelines for animal care and were kept under specific pathogen-free conditions according to Federation of European Laboratory Animal Science Association recommendations. Mice deficient in TLR2, TLR4, TLR2/4, MyD88, Trif, and MyD88/Trif had a C57BL/6 background and have been described previously (82–85). Mice deficient in Rip2 (B6.129S1-Ripk2tm1Flv/J) and miR-155 (B6.Cg-Mir155tm1.1Rsky/J) were purchased from Jackson Laboratories. Mice deficient in MyD88/Trif/Rip2 were generated by crossing MyD88/Trif$^{-/-}$ mice with Rip2$^{-/-}$ mice. As control, WT BMMs were isolated from C57BL/6J mice.

Statistical Analysis. Statistical analyses were performed using Student's *t* test.

ACKNOWLEDGMENTS. We thank Kirstin Hoffmann and Meike Soerensen for excellent technical assistance, and Dr. Daniel Becker and Dr. Kate Holden-Dye for editing the manuscript. MyD88/Trif$^{-/-}$ mice were a gift from the Faculty of Veterinary Medicine, Technical University, Munich. This work was funded by the Sixth Research Framework Programme of the European Union, Project SIROCCO (LSHG-CT-2006-037900) and the Deutsche Forschungsgemeinschaft through SFB633. M.K. was funded by the International Max Planck Research School for Infectious Diseases and Immunology.

1. Parkin DM (2006) The global health burden of infection-associated cancers in the year 2002. *Int J Cancer* 118:3030–3044.
2. Malfertheiner P, Chan FK, McColl KE (2009) Peptic ulcer disease. *Lancet* 374: 1449–1461.
3. Blaser MJ, et al. (1995) Infection with *Helicobacter pylori* strains possessing cagA is associated with an increased risk of developing adenocarcinoma of the stomach. *Cancer Res* 55:2111–2115.
4. Eck M, et al. (1997) MALT-type lymphoma of the stomach is associated with *Helicobacter pylori* strains expressing the CagA protein. *Gastroenterology* 112: 1482–1486.
5. IARC (1994) *IARC Monographs on the Evaluation of Carcinogenic Risks to Humans. Schistosomes, Liver Flukes and* Helicobacter pylori (International Agency for Research on Cancer, Lyon, France).
6. Olbermann P, et al. (2010) A global overview of the genetic and functional diversity in the *Helicobacter pylori* cag pathogenicity island. *PLoS Genet* 6:e1001069.
7. Higashi H, et al. (2002) SHP-2 tyrosine phosphatase as an intracellular target of *Helicobacter pylori* Cag. *Protein Sci* 295:683–686.
8. Churin Y, et al. (2003) *Helicobacter pylori* CagA protein targets the c-Met receptor and enhances the motogenic response. *J Cell Biol* 161:249–255.
9. Tegtmeyer N, et al. (2010) A small fibronectin-mimicking protein from bacteria induces cell spreading and focal adhesion formation. *J Biol Chem* 285:23515–23526.
10. Bartel DP (2009) MicroRNAs: Target recognition and regulatory functions. *Cell* 136: 215–233.
11. Friedman RC, Farh KK-H, Burge CB, Bartel DP (2009) Most mammalian mRNAs are conserved targets of microRNAs. *Genome Res* 19:92–105.
12. Farazi TA, Juranek SA, Tuschl T (2008) The growing catalog of small RNAs and their association with distinct Argonaute/Piwi family members. *Development* 135: 1201–1214.
13. Guo H, Ingolia NT, Weissman JS, Bartel DP (2010) Mammalian microRNAs predominantly act to decrease target mRNA levels. *Nature* 466:835–840.
14. Tili E, Croce CM, Michaille J-J (2009) miR-155: On the crosstalk between inflammation and cancer. *Int Rev Immunol* 28:264–284.
15. Fehri LF, et al. (2010) *Helicobacter pylori* induces miR-155 in T cells in a cAMP-Foxp3-dependent manner. *PLoS ONE* 5.
16. Xiao B, et al. (2009) Induction of microRNA-155 during *Helicobacter pylori* infection and its negative regulatory role in the inflammatory response. *J Infect Dis* 200: 916–925.
17. Lu F, et al. (2008) Epstein-Barr virus-induced miR-155 attenuates NF-kappaB signaling and stabilizes latent virus persistence. *J Virol* 82:10436–10443.
18. Ma X, Becker Buscaglia LE, Barker JR, Li Y (2011) MicroRNAs in NF-kappaB signaling. *J Mol Cell Biol* 3:159–166.
19. Backert S, Naumann M (2010) What a disorder: Proinflammatory signaling pathways induced by *Helicobacter pylori*. *Trends Microbiol* 18:479–486.
20. Hutton ML, et al. (2010) *Helicobacter pylori* exploits cholesterol-rich microdomains for induction of NF-kappaB-dependent responses and peptidoglycan delivery in epithelial cells. *Infect Immun* 78:4523–4531.
21. Bartfeld S, et al. (2010) High-throughput and single-cell imaging of NF-kappa B oscillations using monoclonal cell lines. *BMC Cell Biol* 11:21.
22. Viala J, et al. (2004) Nod1 responds to peptidoglycan delivered by the *Helicobacter pylori* cag pathogenicity island. *Nat Immunol* 5:1166–1174.
23. Rad R, et al. (2009) Extracellular and intracellular pattern recognition receptors cooperate in the recognition of *Helicobacter pylori*. *Gastroenterology* 136:2247–2257.
24. Moran AP (1997) *Helicobacter pylori* lipopolysaccharide (LPS). *Gut* 41(Suppl 3):A18.
25. Monack DM, Raupach B, Hromockyj AE, Falkow S (1996) Salmonella typhimurium invasion induces apoptosis in infected macrophages. *Proc Natl Acad Sci USA* 93: 9833–9838.
26. Gross A, Terraza A, Ouahrani-Bettache S, Liautard JP, Dornand J (2000) In vitro Brucella suis infection prevents the programmed cell death of human monocytic cells. *Infect Immun* 68:342–351.
27. Oldani A, et al. (2009) *Helicobacter pylori* counteracts the apoptotic action of its VacA toxin by injecting the CagA protein into gastric epithelial cells. *PLoS Pathog* 5: e1000603.
28. Buti L, et al. (2011) *Helicobacter pylori* cytotoxin-associated gene A (CagA) subverts the apoptosis-stimulating protein of p53 (ASPP2) tumor suppressor pathway of the host. *Proc Natl Acad Sci USA* 108:9238–9243.
29. Yamasaki E, et al. (2006) *Helicobacter pylori* vacuolating cytotoxin induces activation of the proapoptotic proteins Bax and Bak, leading to cytochrome c release and cell death, independent of vacuolation. *J Biol Chem* 281:11250–11259.
30. Cheng Y, et al. (2005) *Helicobacter pylori*-induced macrophage apoptosis requires activation of ornithine decarboxylase by c-Myc. *J Biol Chem* 280:22492–22496.
31. Menaker RJ, Ceponis PJM, Jones NL (2004) Helicobacter pylori induces apoptosis of macrophages in association with alterations in the mitochondrial pathway. *Infect Immun* 72:2889–2898.
32. Galgani M, et al. (2004) Helicobacter pylori induces apoptosis of human monocytes but not monocyte-derived dendritic cells: Role of the cag pathogenicity island. *Infect Immun* 72:4480–4485.
33. Linnstaedt SD, Gottwein E, Skalsky RL, Luftig MA, Cullen BR (2010) Virally induced cellular microRNA miR-155 plays a key role in B-cell immortalization by Epstein-Barr virus. *J Virol* 84:11670–11678.
34. Gironella M, et al. (2007) Tumor protein 53-induced nuclear protein 1 expression is repressed by miR-155, and its restoration inhibits pancreatic tumor development. *Proc Natl Acad Sci USA* 104:16170–16175.
35. Bolisetty MT, Dy G, Tam W, Beemon KL (2009) Reticuloendotheliosis virus strain T induces miR-155, which targets JARID2 and promotes cell survival. *J Virol* 83: 12009–12017.
36. Kong W, et al. (2010) MicroRNA-155 regulates cell survival, growth, and chemosensitivity by targeting FOXO3a in breast cancer. *J Biol Chem* 285:17869–17879.
37. Levati L, et al. (2009) Altered expression of selected microRNAs in melanoma: Antiproliferative and proapoptotic activity of miRNA-155. *Int J Oncol* 35:393–400.
38. Lu C, et al. (2011) miR-221 and miR-155 regulate human dendritic cell development, apoptosis, and IL-12 production through targeting of p27kip1, KPC1, and SOCS-1. *Blood* 117:4293–4303.
39. O'Connell RM, Taganov KD, Boldin MP, Cheng G, Baltimore D (2007) MicroRNA-155 is induced during the macrophage inflammatory response. *Proc Natl Acad Sci USA* 104: 1604–1609.
40. Yokota S-i, et al. (2007) Highly-purified *Helicobacter pylori* LPS preparations induce weak inflammatory reactions and utilize Toll-like receptor 2 complex but not Toll-like receptor 4 complex. *FEMS Immunol Med Microbiol* 51:140–148.
41. Ishihara S, et al. (2004) Essential role of MD-2 in TLR4-dependent signaling during *Helicobacter pylori*-associated gastritis. *J Immunol* 173:1406–1416.
42. Kawai T, Akira S (2010) The role of pattern-recognition receptors in innate immunity: Update on Toll-like receptors. *Nat Immunol* 11:373–384.
43. Schwartz JT, Allen L-AH (2006) Role of urease in megasome formation and *Helicobacter pylori* survival in macrophages. *J Leukoc Biol* 79:1214–1225.
44. Herskovits AA, Auerbuch V, Portnoy DA (2007) Bacterial ligands generated in a phagosome are targets of the cytosolic innate immune system. *PLoS Pathog* 3:e51.
45. Honda K, et al. (2005) IRF-7 is the master regulator of type-I interferon-dependent immune responses. *Nature* 434:772–777.
46. Kwok T, et al. (2007) Helicobacter exploits integrin for type IV secretion and kinase activation. *Nature* 449:862–866.
47. Shin S, et al. (2008) Type IV secretion-dependent activation of host MAP kinases induces an increased proinflammatory cytokine response to Legionella pneumophila. *PLoS Pathog* 4:e1000220.
48. Lewis BP, Burge CB, Bartel DP (2005) Conserved seed pairing, often flanked by adenosines, indicates that thousands of human genes are microRNA targets. *Cell* 120: 15–20.
49. Rai D, Kim S-W, McKeller MR, Dahia PLM, Aguiar RCT (2010) Targeting of SMAD5 links microRNA-155 to the TGF-beta pathway and lymphomagenesis. *Proc Natl Acad Sci USA* 107:3111–3116.
50. Ceppi M, et al. (2009) MicroRNA-155 modulates the interleukin-1 signaling pathway in activated human monocyte-derived dendritic cells. *Proc Natl Acad Sci USA* 106: 2735–2740.
51. Gottwein E, et al. (2007) A viral microRNA functions as an orthologue of cellular miR-155. *Nature* 450:1096–1099.
52. Asangani IA, et al. (2008) MicroRNA-21 (miR-21) post-transcriptionally downregulates tumor suppressor Pdcd4 and stimulates invasion, intravasation and metastasis in colorectal cancer. *Oncogene* 27:2128–2136.
53. Clop A, et al. (2006) A mutation creating a potential illegitimate microRNA target site in the myostatin gene affects muscularity in sheep. *Nat Genet* 38:813–818.
54. Schulte LN, Eulalio A, Mollenkopf HJ, Reinhardt R, Vogel J (2011) Analysis of the host microRNA response to Salmonella uncovers the control of major cytokines by the let-7 family. *EMBO J* 30:1977–1989.
55. Taganov KD, Boldin MP, Chang KJ, Baltimore D (2006) NF-kappaB-dependent induction of microRNA miR-146, an inhibitor targeted to signaling proteins of innate immune responses. *Proc Natl Acad Sci USA* 103:12481–12486.
56. Volinia S, et al. (2006) A microRNA expression signature of human solid tumors defines cancer gene targets. *Proc Natl Acad Sci USA* 103:2257–2261.
57. Sheridan C, Brumatti G, Elgendy M, Brunet M, Martin SJ (2010) An ERK-dependent pathway to Noxa expression regulates apoptosis by platinum-based chemotherapeutic drugs. *Oncogene* 29:6428–6441.
58. Smythies LE, et al. (2010) Inflammation anergy in human intestinal macrophages is due to Smad-induced IkappaBalpha expression and NF-kappaB inactivation. *J Biol Chem* 285:19593–19604.
59. Lamb A, et al. (2009) Helicobacter pylori CagA activates NF-kappaB by targeting TAK1 for TRAF6-mediated Lys 63 ubiquitination. *EMBO Rep* 10:1242–1249.
60. Reim D, Rossmann-Bloeck T, Jusek G, Prazeres da Costa O, Holzmann B (2011) Improved host defense against septic peritonitis in mice lacking MyD88 and TRIF is linked to a normal interferon response. *J Leukoc Biol* 90:613–620.
61. Auerbuch V, Golenbock DT, Isberg RR (2009) Innate immune recognition of Yersinia pseudotuberculosis type III secretion. *PLoS Pathog* 5:e1000686.
62. Jimenez-Soto LF, et al. (2009) *Helicobacter pylori* type IV secretion apparatus exploits beta 1 integrin in a novel RGD-independent manner. *PLoS Path* 5(12).
63. Sander LE, et al. (2011) Detection of prokaryotic mRNA signifies microbial viability and promotes immunity. *Nature* 474:385–389.
64. Munari F, et al. (2011) Tumor-associated macrophages as major source of APRIL in gastric MALT lymphoma. *Blood* 117:6612–6616.
65. Kaparakis M, et al. (2008) Macrophages are mediators of gastritis in acute Helicobacter pylori infection in C57BL/6 mice. *Infect Immun* 76:2235–2239.
66. Oertli M, et al. (2011) MicroRNA-155 is essential for the T cell-mediated control of *Helicobacter pylori* infection and for the induction of chronic gastritis and colitis. *J Immunol* 187:3578–3586.
67. Hinz M, et al. (2010) A cytoplasmic ATM-TRAF6-cIAP1 module links nuclear DNA damage signaling to ubiquitin-mediated NF-κB activation. *Mol Cell* 40:63–74.
68. Okamura S, et al. (2001) p53DINP1, a p53-inducible gene, regulates p53-dependent apoptosis. *Mol Cell* 8:85–94.

69. Peng M, Litman R, Jin Z, Fong G, Cantor SB (2006) BACH1 is a DNA repair protein supporting BRCA1 damage response. *Oncogene* 25:2245–2253.
70. Brachat A, et al. (2002) A microarray-based, integrated approach to identify novel regulators of cancer drug response and apoptosis. *Oncogene* 21:8361–8371.
71. Saito Y, et al. (2006) Absence of CD9 enhances adhesion-dependent morphologic differentiation, survival, and matrix metalloproteinase-2 production in small cell lung cancer cells. *Cancer Res* 66:9557–9565.
72. Yunta M, Lazo PA (2003) Apoptosis protection and survival signal by the CD53 tetraspanin antigen. *Oncogene* 22:1219–1224.
73. Eitz Ferrer P, et al. (2011) Induction of Noxa-mediated apoptosis by modified vaccinia virus Ankara depends on viral recognition by cytosolic helicases, leading to IRF-3/IFN-β-dependent induction of pro-apoptotic Noxa. *PLoS Pathog* 7:e1002083.
74. Mimuro H, et al. (2007) *Helicobacter pylori* dampens gut epithelial self-renewal by inhibiting apoptosis, a bacterial strategy to enhance colonization of the stomach. *Cell Host Microbe* 2:250–263.
75. Davies GR, Rampton DS (1994) *Helicobacter-pylori*, free-radicals and gastroduodenal disease. *Eur J Gastroenterol Hepatol* 6(1):1–10.
76. Miyazawa M, et al. (2003) Suppressed apoptosis in the inflamed gastric mucosa of *Helicobacter pylori*-colonized iNOS-knockout mice. *Free Radic Biol Med* 34:1621–1630.
77. Lonkar P, Dedon PC (2011) Reactive species and DNA damage in chronic inflammation: Reconciling chemical mechanisms and biological fates. *Int J Cancer* 128:1999–2009.
78. Collins HL, Schaible UE, Ernst JD, Russell DG (1997) Transfer of phagocytosed particles to the parasitophorous vacuole of *Leishmania mexicana* is a transient phenomenon preceding the acquisition of annexin I by the phagosome. *J Cell Sci* 110:191–200.
79. Wunder C, et al. (2006) Cholesterol glucosylation promotes immune evasion by *Helicobacter pylori*. *Nat Med* 12:1030–1038.
80. Nilsson I, Shabo I, Svanvik J, Monstein HJ (2005) Multiple displacement amplification of isolated DNA from human gallstones: Molecular identification of Helicobacter DNA by means of 16S rDNA-based pyrosequencing analysis. *Helicobacter* 10:592–600.
81. Livak KJ, Schmittgen TD (2001) Analysis of relative gene expression data using real-time quantitative PCR and the 2(-Delta Delta C(T)) Method. *Methods* 25:402–408.
82. Takeuchi O, et al. (1999) Differential roles of TLR2 and TLR4 in recognition of gram-negative and gram-positive bacterial cell wall components. *Immunity* 11:443–451.
83. Hoshino K, et al. (1999) Cutting edge: Toll-like receptor 4 (TLR4)-deficient mice are hyporesponsive to lipopolysaccharide: Evidence for TLR4 as the Lps gene product. *J Immunol* 162:3749–3752.
84. Adachi O, et al. (1998) Targeted disruption of the MyD88 gene results in loss of IL-1- and IL-18-mediated function. *Immunity* 9:143–150.
85. Hoebe K, Du X, Goode J, Mann N, Beutler B (2003) Lps2: A new locus required for responses to lipopolysaccharide, revealed by germline mutagenesis and phenotypic screening. *J Endotoxin Res* 9:250–255.